Water Research 218 (2022) 118517

Contents lists available at ScienceDirect

Water Research

journal homepage: www.elsevier.com/locate/watres

Microbial response on the first full-scale DEMON® biomass transfer for mainstream deammonification

Sabine Marie Podmirseg [a,b,*], María Gómez-Brandón [a,b,c], Markus Muik [a], Blaz Stres [d,e], Martin Hell [f], Thomas Pümpel [a], Sudhir Murthy [g], Kartik Chandran [h], Hongkeun Park [h], Heribert Insam [a], Bernhard Wett [i]

[a] Department of Microbiology, University of Innsbruck, Technikerstraße 25d, 6020 Innsbruck, Austria
[b] alpS GmbH, Grabenweg 68, 6020 Innsbruck, Austria
[c] Grupo Ecoloxía Animal (GEA), Centro di Investigación Mariña (CIM), Universidade de Vigo, E-36310, Spain
[d] University of Ljubljana, Biotechnical Faculty, Jamnikarjeva 101, 1000 Ljubljana, Slovenia
[e] University of Ljubljana, Faculty of Geodetic and Civil Engineering, Jamova 2, 1000 Ljubljana, Slovenia
[f] Achental-Inntal-Zillertal Water Board, Hausnummer 150, 6261 Strass i.Z., Austria
[g] NEWhub Corp, 12602 Denmark Drive, Herndon, VA 20171
[h] Department of Earth and Environmental Engineering, Columbia University, 500 West 120th Street, NY 10027, United States
[i] ARAconsult GmbH, Unterbergerstraße 1, 6020 Innsbruck, Austria

ARTICLE INFO

Keywords:
Wastewater treatment
Activity tests
Microbial community
Heme quantification
Partial nitritation anammox

ABSTRACT

Sidestream partial nitritation and deammonification (pN/A) of high-strength ammonia wastewater is a well-established technology. Its expansion to the mainstream is, however mainly impeded by poor retention of anaerobic ammonia oxidizing bacteria (AnAOB), insufficient repression of nitrite oxidizing bacteria (NOB) and difficult control of soluble chemical oxygen demand and nitrite levels.

At the municipal wastewater treatment plant in Strass (Austria) the microbial consortium was exhaustively monitored at full-scale over one and a half year with regular transfer of sidestream DEMON® biomass and further retention and enrichment of granular anammox biomass via hydrocyclone operation.

Routine process parameters were surveyed and the response and evolution of the microbiota was followed by molecular tools, *ex-situ* activity tests and further, AnAOB quantification through particle tracking and heme measurement.

After eight months of operation, the first anaerobic, simultaneous depletion of ammonia and nitrite was observed *ex-situ*, together with a direction to higher nitrite generation (68% of total NO_x-N) as compared to nitrate under aerobic conditions. Our dissolved oxygen (DO) scheme allowed for transient anoxic conditions and had a strong influence on nitrite levels and the NOB community, where *Nitrobacter* eventually dominated *Nitrospira*. The establishment of a minor but stable AnAOB biomass was accompanied by the rise of *Chloroflexi* and distinct emergence of *Chlorobi*, a trend not seen in the sidestream system. Interestingly, the most pronounced switch in the microbial community and noticeable NOB repression occurred during unfavorable conditions, i.e. the cold winter season and high organic load. Further abatement of NOB was achieved through bioaugmentation of aerobic ammonia oxidizing bacteria (AerAOB) from the sidestream-DEMON® tank. Performance of the sidestream pN/A was not impaired by this operational scheme and the average volumetric nitrogen removal rate of the mainstream even doubled in the second half of the monitoring campaign. We conclude that a combination of both, regular sidestream-DEMON® biomass transfer and granular SRT increase via hydrocyclone operation was crucial for AnAOB establishment within the mainstream.

* Corresponding author at: University of Innsbruck, Department of Microbiology, Technikerstraße 25d, 6020 Innsbruck, Austria.
E-mail addresses: sabine.podmirseg@uibk.ac.at (S.M. Podmirseg), markus.muik@a1.net (M. Muik), hell@aiz.at (M. Hell), thomas.puempel@uibk.ac.at (T. Pümpel), kc2288@columbia.edu (K. Chandran), ppark@ocsan.gov (H. Park), heribert.insam@uibk.ac.at (H. Insam), wett@araconsult.at (B. Wett).

https://doi.org/10.1016/j.watres.2022.118517
Received 18 August 2021; Received in revised form 16 April 2022; Accepted 24 April 2022
Available online 27 April 2022

1. Introduction

The identification of anaerobic ammonia oxidizing bacteria (AnAOB) by Strous and co-workers in 1999 (Strous et al., 1999a) not only confirmed the long-time postulated existence of such a microbial group (Broda, 1977), thus closing the gap in the nitrogen cycle, but also led to a fast evolution of ground breaking wastewater treatment strategies (i.e. DEMON®; SHARON-Anammox known as single reactor system for high activity removal over nitrite - anaerobic ammonium oxidation; ANITA™ MOX; DEAMOX - DEnitrifying AMonium Oxidation - among others) (Christensson et al., 2013; Kalyuzhnyi et al., 2008; van Dongen et al., 2001; Wett et al., 2007). The involved *Planctomycetes* of the order *Brocadiales* encompass as for today five different genera, i.e. '*Candidatus* Kuenenia', '*Ca.* Brocadia', '*Ca.* Anammoxoglobus', '*Ca.* Jettenia' *and* '*Ca.* Scalindua' and several novel clades that have yet not been completely described and affiliated (Jetten et al., 2009; Mardanov et al., 2019; Shehzad et al., 2016; Sun et al., 2014). Thorough investigations during the last twenty years have substantially uncovered their physiological needs and structural properties, helping to adjust optimal operational conditions (Ali et al., 2020; Kartal et al., 2012; Liu et al., 2020; Strous et al., 1999b; Szatkowska and Paulsrud, 2014; van Niftrik and Jetten, 2012). Nowadays, the process of nitrogen elimination through deammonification, i.e. partial nitritation by aerobic ammonia oxidizing microorganisms (AerAOM; i.e. ammonia oxidizing bacteria (AerAOB) and archaea (AerAOA)) followed by anaerobic ammonia oxidation through AnAOB is ideally suited for treatment of high-strength ammonium wastewaters such as anaerobic sludge liquor. Since the first start-up and effective implementation of the pH-controlled DEMON® process at the wastewater treatment plant (WWTP) in Strass in 2004 (Wett, 2007), ca. 100 full-scale DEMON® plants are in operation worldwide or under design or construction and the basic process strategy of pN/A is implemented in ca. 200 full-scale facilities worldwide (Lackner et al., 2014; WEF/WERF, 2015).

After a decade of successful sidestream treatment of ammonia-rich wastewaters, the scope of the anammox process has been expanded essentially in laboratory-scale experiments to low-strength ammonia wastewater and moderate- or low-temperature ranges (De Clippeleir et al., 2011; Hendrickx et al., 2012; Hoekstra et al., 2019; Kamp et al., 2019; Le et al., 2019; Yeshi et al., 2016). The effect on the microbial composition was explored utilizing pilot-plants and mostly short-term monitoring (Hoekstra et al., 2019; Wang et al., 2016; Yang et al., 2018). Still, there are considerable drawbacks hampering an effective implementation in the mainstream, such as insufficient AnAOB biomass retention, ineffective inhibition of nitrite oxidizing bacteria (NOB), the successful containment of denitrifier growth, or soluble chemical oxygen demand (COD) availability (Li et al., 2018; Xu et al., 2015; Zhang et al., 2019). In addition, the influence and widespread presence of newly identified bacteria involved in complete ammonia oxidation (comammox) is being increasingly recognized (Annavajhala et al., 2018; Daims et al., 2015; Gottshall et al., 2021).

In this study we present the results of a one and a half year full-scale monitoring campaign introducing the deammonification process to the mainstream of a municipal WWTP. To allow for an ideal initiation of the deammonification process in the low-rate biological stage (B-stage), constant seeding of AnAOB and AerAOM biomass from the sidestream DEMON® (i.e. sludge liquor; SL) was performed and the retention time of granular AnAOB biomass in the mainstream was increased by a density-selecting hydrocyclone. The direction towards a nitritation/anammox- rather than a nitrification/denitrification process was further promoted through a specific aeration regime in the mainstream that is summarized together with other operational characteristics in (Wett et al., 2015). In principle, varying dissolved oxygen (DO) levels due to intermittent aeration regime favor AerAOM over NOB due to their different oxygen affinities. Their different nitrite half-saturation characteristics and temperature sensitivities enable the control of competition between NOB and AnAOB.

A comprehensive microbiological monitoring campaign was undertaken collecting not only basic process data but also investigating qualitative and quantitative effects of the novel operational scheme on the microbial consortium. We used quantitative polymerase chain reaction (qPCR), denaturing gradient gel electrophoresis (DGGE), amplicon sequencing, particle tracking and a novel heme quantification kit for on-site AnAOB abundance and activity measurement. Here, we focused on the following points: (i) the effect of DEMON®-biomass seeding on mainstream microbial diversity and activity, (ii) the efficiency of this novel operational scheme to inhibit NOB and thus facilitate mainstream deammonification and (iii) the suitability and contribution of hydrocyclone retention to maintain a constant anammox biomass in the mainstream.

2. Material and methods

2.1. Wastewater treatment plant characteristics and operational scheme

The WWTP AIZ in Strass (Austria; http://aiz.at) is a net energy positive plant performing mainstream treatment through high-rate (A-stage) and low-rate (B-stage) biological stages and it is designed for a population equivalent (PE) load of 167,000 (nitrification/denitrification). The WWTP is located in a typical tourist region, leading to sudden and significant increases in PE loads, especially peaking during the winter holiday season. To alleviate this problem, the DEMON® process was implemented for sidestream treatment of ammonia-rich AD-sludge liquor in 2004. To test the full-scale approach of mainstream deammonification, the plant was adapted to allow for biomass transfer between side- and mainstream (sludge liquor (SL) and biological stage (B), respectively; see Figure S1 or ((Wett et al., 2015); Fig. 1). DEMON® biomass transfer to the mainstream was performed in two ways. Firstly, semi-continuously and in varying amounts in the form of mixed-liquor seeding (AnAOB and AerAOM biomass with no size selection), depending on biomass availability (Fig. 1). Secondly, on a regular basis through the transfer of the overflow (OF) low-density hydrocyclone fraction (usually 1 h of cyclone operation per sequencing batch reactor (SBR) cycle, 4 SBR cycles/day) of the DEMON® tank (mostly AerAOM, AnAOB and little NOB). Increase of anammox sludge retention time in the mainstream was achieved through the installation of a hydrocyclone in the return sludge line to keep the high-density fraction containing anammox granules in the basin. For a further optimization of the process conditions towards a nitritation and mainstream deammonification process, oxygen competition (AerAOB and NOB) and nitrite competition (AnAOB and NOB) were controlled; details can be found in (Wett et al., 2015). A detailed summary on influent parameters – volumetric-, COD-

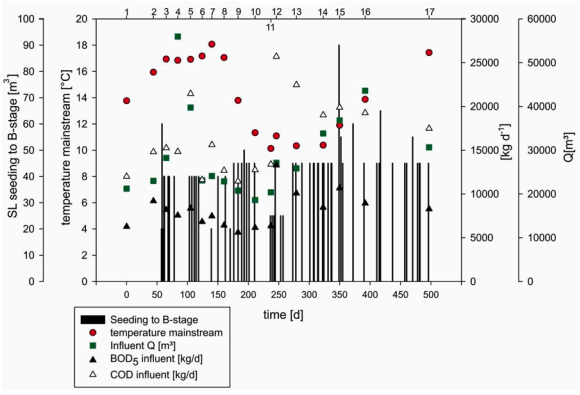

Fig. 1. General WWTP and operational characteristics including influent load Q, influent COD and BOD_5, seeding from the DEMON® to the mainstream and mainstream temperature throughout the whole sampling campaign. The lower X-Axis depicts the time-frame of the whole monitoring campaign in days and the upper X-Axis highlights the seventeen sampling events.

and biological oxygen demand (BOD_5)-loads, seeding load from the side- to the mainstream and mainstream temperature evolution over the whole sampling campaign is depicted in Fig. 1. Additionally, general influent concentrations of the mainstream B-stage (COD load, N_{tot}, NH_4-N, NO_3-N) over the whole sampling campaign are shown in Fig. 2.

2.2. Sampling

The full-scale mainstream deammonification study was monitored on-site by WWTP routine parameters and 17 sampling events over the full test period of 497 days. The series was launched with a control sampling in spring prior to any DEMON® biomass seeding to the mainstream (sampling 1) and finished in autumn of the subsequent year (sampling 17). Samplings 2–6 were in the summer period (mid of June to end of August) and reflect the initiation phase, followed by a low-strain (Q) phase (samplings 7–10, mid of September to end of November). Samplings 11 and 12 depict the high-strain winter holiday season with drastic and rapid increases in PE loads, and the last five samplings (13–17) completed the monitoring campaign until September of the following year. Both, mainstream (B) and sidestream DEMON® samples (SL) were collected. Refer to the supplementary material for more details on sampling times (Table S1) and sampling strategy.

2.3. Physico-chemical analyses

Electrical conductivity (EC) and pH were determined with a conductivity meter (LF 330 WTW; Weilheim, Germany) and a pH meter (Metrohm 744, Herisau, Switzerland), respectively. The dissolved organic matter DOM_{ms} (a_{365}/a_{250}) was estimated from the ratio of the absorbances at 250 and 365 nm, measured with a U-2001 UV/Vis -spectrophotometer (Hitachi, Tokyo, Japan) in centrifuged (5 min at 5000 g) samples. According to (Lindell et al., 1995), an increasing $1/DOM_{ms}$ ratio indicates degradation of dissolved humic substances to smaller organic molecules. Routine plant parameters were monitored according to standard procedures by the AIZ waterboard and were included in this study: Q [m^3], COD [kg d^{-1}], BOD_5 [kg d^{-1}], N_{tot}, NH_4^+-N, NO_2^--N and NO_3^--N all [mg N L^{-1}], and the COD/N ratio for the intermediate clarifier.

2.4. Activity measurements

The potential specific anammox activity was quantified indirectly by *ex-situ* tests determining inorganic nitrogen conversion rates. Anaerobic and aerobic activity tests were performed at room temperature (21.1 ± 1.7 °C) for 120 and 45 min, respectively, with initially spiked ($NaNO_2$ resulting NO_2-N ca. 50 mg L^{-1} and NH_4Cl resulting NH_4-N ca. 40 mg L^{-1}), pH-monitored mainstream samples that were first covered with a floating-lid (i.e. no headspace) and incubated at hypoxic condition (DO-level < 0.1 mg L^{-1}) and thereafter aerated to 3 mg L^{-1} < DO < 5 mg L^{-1}, according to (Wett et al., 2015). Activity rates were calculated for NH_4-, NO_2- and NO_3-N during time periods with unlimited substrate availability (i.e. linear concentration trends) and are given as Δmg g^{-1} TS h^{-1} for each N-species.

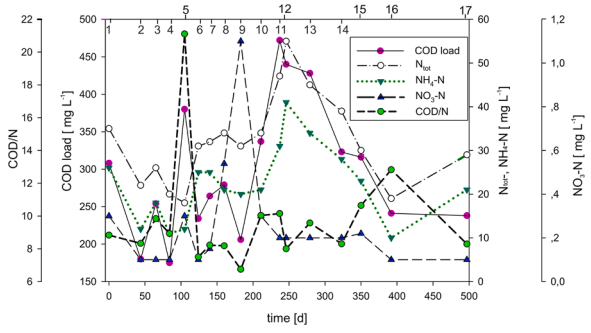

Fig. 2. Concentration of N_{tot}, NH_4-N, NO_3-N, and COD load and COD/N ratio of the intermediate clarifier, i.e. before entering the B-stage, over the whole experimental period. The lower X-Axis depicts the elapsed time in days and the upper X-Axis highlights the seventeen sampling events.

2.5. Particle tracking

Particle tracking was conducted through an image analysis to determine the number of anammox granules mL^{-1} sample in SL- and B-samples as well as in the hydrocyclone underflow (UF) and overflow (OF) fractions thereof. It was further used to estimate the total cross-section area as a proxy for granular anammox mass, displayed as area [mm^2 mL^{-1}] and to capture the distribution of granule size fractions (five radius size categories: < 0.1 mm (category 1); 0.1–0.2 mm (category 2); 0.2–0.3 mm (category 3); 0.3–0.4 mm (category 4) and > 0.4 mm (category 5)). The open source software Fiji (www.fiji.sc) was used, and all calculations were performed according to the protocol described in (Podmirseg et al., 2015).

2.6. Heme quantification

Heme, especially enriched in AnAOB-biomass and a biomarker for anammox presence and -activity (Ali et al., 2013; Podmirseg et al., 2015), was performed for all B-UF and SL-UF samples and for some selected samples of the B-stage with the LCK-cuvette test 411 - Anammox activity (Hach Lange GmbH, Germany), which is based on (Podmirseg et al., 2015). More details can be found in the supplementary material.

2.7. DNA-extraction

Total DNA was extracted using the Qiagen DNeasy® Blood & Tissue Kit (Qiagen, Germany) according to the manufacturer's protocol, with the following modifications in order to improve the DNA yield: an initial sample volume of 1 mL was used for the extraction; the lysis buffer contained 20 mg lysozyme mL^{-1} lysis buffer; the incubation step with proteinase K was prolonged to three hours at 56 °C; each centrifugation step specified in the protocol with ≥ 6000 g was performed at 8000 g and the final elution using buffer AE was performed in two subsequent steps with 50 µL each. DNA extracts were stored in low-DNA binding tubes (Genuine Axygen Quality 1.7 mL Maximum recovery, Axygen Inc., USA) at −20 °C until use.

2.8. Quantitative PCR

Quantitative real-time PCR analysis was performed according to (Podmirseg et al., 2015) to determine the 16S rRNA gene copy numbers of AnAOB. The groups of AerAOB, NOB (*Nitrobacter* spp. (Nb) and *Nitrospira* spp. (Ns) separately) and total bacteria were analysed alike. For the primers and reference microorganisms see Table S2. For qPCR cycling conditions refer to Table S3 and for end-point PCR for stock generation to Table S4. AerAOA were not quantified in this study, as AerAOB are considered the quantitatively more abundant group of AerAOM (Bai et al., 2012).

2.9. Molecular fingerprinting via denaturing gradient gel electrophoresis (PCR-DGGE)

For DGGE analyses amplification of the 16S rRNA gene of AnAOB, AerAOB, Nb and Ns was performed and gels prepared according to (Podmirseg et al., 2019). PCR conditions and gel gradients are summarized in Table S2 and cycling conditions given in Table S4. Diversity of each specific group was evaluated based on band counts (i.e. number of key players within a microbial guild) and similarity of samples analysed via hierarchical clustering of banding patterns.

2.10. 16S rRNA gene amplicon sequencing and data processing

To overview the evolution of the bacterial community in the B and SL samples, specific sampling points were chosen, or combined into sample groups, representing specific experimental phases: 1) control B1; 2) early phase (composite of B3-B5), 3) low-strain phase (B7-B10); 4) high-strain phase (B11 and B12); 5) final monitoring phase (B15-B17); and two time points of the SL samples: 6) early phase (SL1 and SL2) and 7) high-strain phase (SL11 and SL12). For each composite sample extracts were combined in equal amounts adding up to > 1000 ng DNA. The sequencing was conducted on an Ion Torrent Personal Genome Machine using the Ion PGM™ Sequencing 250 Kit and the primer pair 1055F/1392R (see Table S2) targeting the V7–8 region of the bacterial 16S rRNA gene.

Obtained raw reads with minimum sequence lengths of 200 bp were analysed with the CoMA pipeline (Hupfauf et al., 2020), according to (Podmirseg et al., 2019) and datasets subsampled according to the sample with the lowest read number (i.e. 45,291 reads, B3–5).

2.11. Data- and statistical analyses

Multivariate analyses were conducted with the PAST software (Version 2.17) (Hammer et al., 2001). Basically, PCA, PCoA, ANOVA, Kruskal Wallis analysis, NP-MANOVA, correlation-, and fingerprint analysis of DGGE data were performed to screen for significant differences and to monitor the evolution of the microbial communities. For detailed information on each specific statistical test and respective data set that was analysed please refer to the supplementary material.

3. Results

3.1. General evaluation of the process scheme

Basic data on the influent characteristics and environmental conditions are depicted in Fig. 1 and Figure S2 (daily values) and Table S1, and can be summarized as follows: the average temperature during the sampling period was 14.1 ± 3.1 °C with a minimum value of 8.1 °C and maximum of 19 °C. The pH was 7.31 ± 0.31 and 7.74 ± 0.25 in the mainstream and DEMON® sidestream, respectively. Mean electrical conductivity in the B-stage was 0.72 ± 0.14 mS cm^{-1}, while it was significantly higher in the SL reactor (3.01 ± 0.52 mS cm^{-1}). The 1/DOM_{ms} measurement indicated a stronger presence of higher molecular size compounds in the SL as compared to B, with values of 3.58 ± 0.62 and 10.8 ± 3.24, respectively.

Influent load during the sampling campaign ranged from 17,133 to 108,400 $m^3\ d^{-1}$ with a mean of 29,490 ± 10,752 $m^3\ d^{-1}$. The COD- and BOD_5 influent loads were 15,773 ± 4826 kg d^{-1}, and 7930 ± 2379 kg d^{-1}, respectively. Total nitrogen concentration was 39.2 ± 11.5 mg L^{-1}, peaking at 69 mg L^{-1} (Fig. 2). A total of 3010 m^3 of sidestream biomass was bioaugmented to the mainstream in 73 events of 15 to 90 m^3 per day.

Fig. 2 summarizes the B-stage influent concentrations (COD load, COD/N, total N-, NH_4-N- and NO_3-N-influent) that were measured in the intermittent clarifier. Higher organic- (samplings 5 and 11–13) and nitrogen concentrations (samplings 11–13) as well as a peak in nitrate at time point 9 can be seen.

Higher total nitrogen concentrations and loads in the influent caused a response mainly in the oxidised nitrogen species, with a slight temporal shift (Fig. 3). Ammonia effluent concentrations remained stable over the whole period with average values of 2.9 ± 1.4 mg L^{-1} and extreme values of 0.3 and 10.6 mg L^{-1}. This indicates that a stable nitrification performance was achieved that had to cope with sudden load pulses (e.g. holiday season around sampling B12). Nitrite levels were very low from time point B1 to B10 and showed a tenfold increase around sampling point B11 and B12 from 0.32 to 4.05 mg L^{-1} until they decreased around B14 and stabilized at initial values around sampling

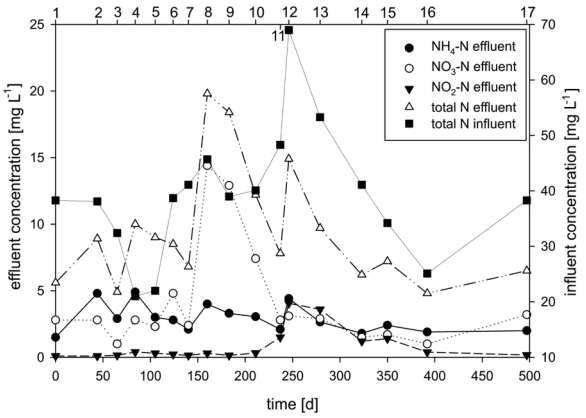

Fig. 3. Concentration of total nitrogen in the influent throughout the monitoring phase (right Y-Axis) and effluent characteristics for total bound nitrogen and the three nitrogen species NH_4-, NO_2- and NO_3-N, respectively (left Y-Axis). The lower X-Axis depicts the elapsed time in days and the upper X-Axis highlights the seventeen sampling events.

B16. Finally, nitrate was the most fluctuating nitrogen species, reaching highest values during sampling period B8 to B10 and B12. Concentrations ranged around 4.1 ± 3.9 mg L^{-1} with extremes of 1.0 and 14.4 mg L^{-1}. Decrease in nitrate-concentration co-occurs with nitrite-increase in the period between day 200 and 250 and nitrite overshoots nitrate at the point of time when the Christmas load-peak was received (B12).

Nitrogen removal efficiency (N-RE) and ammonium removal efficiency (NH_4-N RE) of the mainstream averaged 84.1% ± 11.1% and 68.6% ± 15.1%, respectively with highest values achieved at B1 and during samplings B11-B14 (see supplementary Table S7). The mainstream volumetric nitrogen removal rate reached 58.4 ± 24.5 g N $m^{-3}\ d^{-1}$ and biomass-specific NRR 13.9 ± 5.2 mg N g^{-1} TSS d^{-1}, respectively. A clear increase in NRR from sampling B10 to B15 was detectable and maxima reached 104 g N $m^{-3}\ d^{-1}$ at B14 and 27.5 mg N g^{-1} TSS d^{-1} at B15, respectively (Table S7).

3.2. Particle tracking

Based on the characteristic reddish color of the AnAOB granules, particle tracking allowed for a detailed insight into the bioaugmentation of the mainstream with DEMON® biomass and the retention strategy through hydrocyclone operation (Podmirseg et al., 2015) (Figure S3). Throughout the sampling period, AnAOB biomass was increased and successfully maintained in the mainstream. The initial (B1) anammox abundance in the mainstream was 0.33 ± 0.42 particles mL^{-1} with a total cross-section area of 0.031 ± 0.05 $mm^2\ mL^{-1}$. Detected anammox granules could only be assigned to the smallest size categories 1 and 2. Until sampling B4, a constant increase of anammox biomass (area) was noticed followed by a stabilization phase (B5-B9) and a subsequent strong increase (B10–12), until the anammox biomass reached its peak at sampling time B12 with 6.17 granules mL^{-1} and 3.02 $mm^2\ mL^{-1}$, respectively. Here, 24% of all granules could be attributed to size categories 3–5 (15.2% (category 3), 5.29% (category 4) and 3.57% (category 5)). The particle number peaked at sampling B13 with 23.7 granules mL^{-1}, but due to fewer big granules (only 2.77% in categories 3–5), the overall anammox biomass (area) dropped considerably. In the end (B17) 15.6 ± 9.03 granules were detected per mL and the granules' cross-section area ranged around 0.4 ± 0.29 $mm^2\ mL^{-1}$, similar to the stabilization phase (B5-B9). Finally, 3.18% of the granules were within size categories 3–5. Compared to the control sampling (B1) prior to bioaugmentation, anammox biomass (area) was increased 17 times until B17 and even 97 times at the peak B12. Similarly, for granule abundance, a 47- fold and even 72-fold increase, compared to control levels, was achieved at B17 and B13, respectively.

The hydrocyclone clearly selected for bigger granules in the underflow, as (i) no granules of size category 5 were detected in the B-OF fraction or very few at the SL-stage; (ii) the smallest size category was most abundant in the overflow fraction, followed by the sample origin (B or SL) and eventually the underflow-fraction; and last (iii) particle concentrations were considerably higher in the underflow (Table S5).

3.3. Activity measurements

Ex-situ anaerobic and aerobic activity measurements of the B-stage were conducted to shed light onto the evolution of the potential nitrogen turnover rates. The potential activity of specific groups and pathways that can occur simultaneously could be determined following the underlying principles: Firstly, concerning anoxic incubation the potential ammonification of dissolved organic nitrogen leads to an increase (NH_4-N ↑) and activity of AnAOB to a decrease of ammonium (NH_4-N ↓); both AnAOB- and denitrifier-activity lower nitrite concentration (NO_2-N ↓) and AnAOB-activity slightly increases nitrate concentration (NO_3-N ↑), while potential denitrifier activity leads to nitrate decrease (NO_3-N ↓). Secondly, *aerobic incubation* permits AerAOB-activity with nitrite- (NO_2-N ↑) and NOB-activity with concomitant nitrate-increase (NO_3-N ↑); here nitrite accumulation points out imbalances in the activity of the nitrifier community. Measurements were carried out starting from sampling point 5 (day 105). Initially, the anaerobic activity measurements showed concurrent nitrite and nitrate removal (NO_x-$N < 0.75$ mg N g^{-1} TSS h^{-1}) and ammonium increase at low levels (Fig. 4; left). These low rates were preserved, under temporary nitrite generation (B8, B10). After sampling B10 the trends changed drastically towards clearly reduced ammonium generation (except for B13) and even net ammonium removal at samplings B12, B14 and B15. Nitrite depletion rates increased 5 to even 24-fold the average depletion rate of interval B5-B10. In general, after B12, nitrite depletion was significantly higher than nitrate removal (ratio on average 4.6 to 1). The highest removal rates for all nitrogen species were −0.05 mg NH_4-N g^{-1} TSS h^{-1} (B15), −3.84 mg NO_2-N g^{-1} TSS h^{-1} (B15) and- 1.13 mg NO_3-N g^{-1} TSS h^{-1} (B15). The first simultaneous net ammonium and nitrite removal was detected at sampling B12.

The general trends for aerobic activity measurements can also be grouped into the first six (B5-B10) and the last six (B12-B17) sampling points (Fig. 4; right). At the beginning, full conversion of ammonium towards nitrate was observed (−1.24 mg NH_4-N g^{-1} TSS h^{-1} to 1.43 mg NO_3-N g^{-1} TSS h^{-1}). These average ammonium oxidation rates remained relatively stable with eventual accessorily nitrite depletion. However, at sampling point B12 the general picture changed and nitrate generation was repressed. On average, for the last five sampling times (B13-B17), ammonium depletion doubled, a drastic increase in nitrite generation was recorded and nitrate generation was cut in half. The highest removal rates for ammonium and generation of nitrite were −5.59 mg N g^{-1} TSS h^{-1} (B15) and 5.37 mg N g^{-1} TSS h^{-1} (B15), respectively and the lowest production of NO_3-N was encountered at sampling B16 (0.6 mg N g^{-1} TSS h^{-1}). For the first time at sampling B12 and thereafter (except for sampling B13) more ammonium was converted to nitrite, compared to nitrate, with average values of 68.3 ± 16% (total NO_x-N) and the highest generation of nitrite with 83.2% (total NO_x-N) at B15.

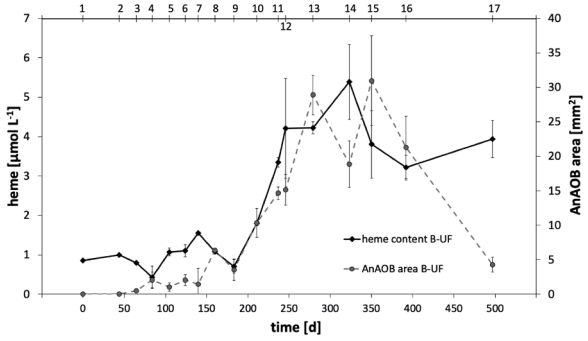

Fig. 4. Activity measurement of mainstream samples during anaerobic (left) and aerobic incubation (right) at ambient temperature. Activities are defined as NH_4-, NO_2- and NO_3-N turnover per g total dissolved solids (TSS) per hour. Extended and modified data set as found in (Wett et al., 2013).

3.4. Heme quantification

An additional non-molecular quantification strategy for the AnAOB biomass, the heme measurement (Podmirseg et al., 2015) was chosen. Selected samples of the B-stage showed a range of 0.12 to 1.13 ± 0.07 µmol L^{-1} heme, with an initial small peak right after the bio-augmentation had started (B2) and followed by an eventual increase at the samplings B10 and B11 (Figure S6). The final value (B17) was comparable to that from sampling B2. Heme content in SL-UF, averaged 42 ± 25 µmol L^{-1} with lowest and highest values of 13 and 71.3 µmol L^{-1}, respectively (Figure S6). Due to reproducible operation conditions of the hydrocyclone, the evolution of the relative heme abundance of B-UF and B-samples should follow a similar trend. Therefore, and also because of B-sample shortage, B-UF heme was compared with AnAOB gene abundance (16S rRNA gene copy numbers) (Figure S7) and AnAOB cross section area of B-UF-samples (particle tracking) (Fig. 5). Correlation analyses rendered significant coefficients of $r = 0.52$ and $r = 0.77$ for both pairs, respectively ($p<0.05$) (see Table S6) and general trends were comparable among investigated parameters, with the exception of AnAOB gene abundance already showing one extra peak at B4, whereas in general an increase of all parameters was occurring around sampling B10-B13.

Further significant and positive correlation of heme could be detected for AnAOB area B, AerAOB and NO_2-N concentrations in the mainstream, with values of 0.681, 0.553 and 0.657, respectively (Table S6).

3.5. Quantification of involved nitrifiers

The quantitative community dynamics of the most important groups, i.e. AnAOB, AerAOB, NOB (Nb and Ns) and total bacteria are shown in Fig. 6. The total bacterial abundance remained stable with some minor drops during low-strain phases and averaged $1.1 \times 10^9 \pm 6.2 \times 10^8$ gene copies mL^{-1} in the mainstream. The AerAOB population exhibited a similar pattern until population constantly rose from B11 onwards and eventually reached 46-fold values of the B1 AerAOB population. AnAOB abundance initially (B1) was below the detection limit of 1.2×10^4 gene

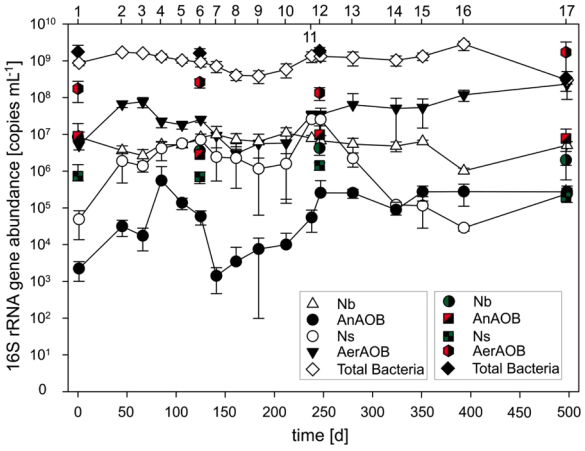

Fig. 5. Evolution of heme concentration [µmol L^{-1}] of the mainstream cyclone underflow fraction (B-UF) over the whole sampling campaign as compared to the evolution of AnAOB area of B-samples determined via particle tracking method. Numbers on the top indicate respective sampling points.

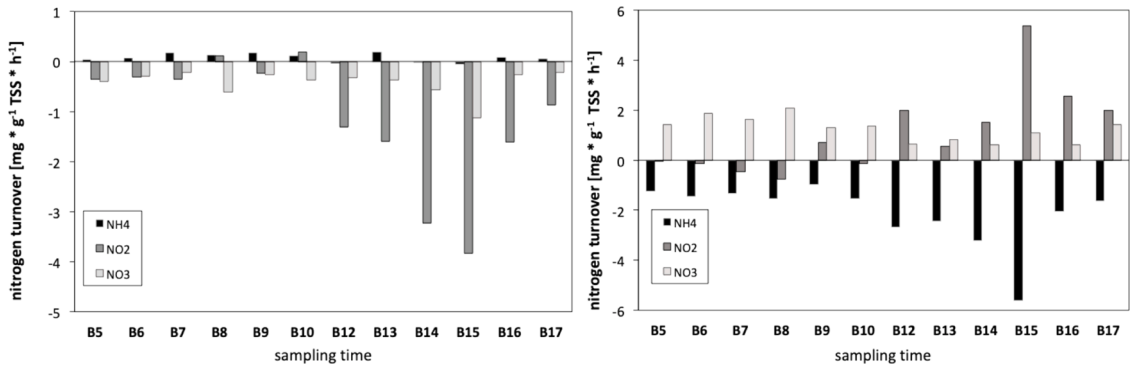

Fig. 6. Quantitative analysis of 16S rRNA genes of total bacteria, AerAOB, AnAOB, *Nitrobacter* and *Nitrospira* over the whole sampling period. The lower X-Axis depicts the time-frame of the whole monitoring campaign in days and the upper X-Axis highlights the seventeen sampling events. Coloured symbols at sampling time 1, 6, 12 and 17 reflect the results of side-stream SL-samples.

copies mL^{-1}. It increased thereafter with the characteristic drop during the low-strain phase as described for the earlier mentioned groups. From sampling B12 onwards, AnAOB levels stabilised around $2.38 \times 10^5 \pm 7.35 \times 10^4$ gene copies mL^{-1}. The SL AnAOB values were constantly higher ($7.32 \times 10^6 \pm 3.10 \times 10^6$ gene copies mL^{-1}). The *Nitrobacter* population remained relatively stable over time in the mainstream and dominated the sidestream NOB community with on average 7.4 fold higher gene copy values than *Nitrospira*. In the mainstream the predominance over *Nitrospira* was persistent apart from sampling B11 and B12, where *Nitrospira* experienced a drastic increase to values of $2.6 \times 10^7 \pm 3.96 \times 10^6$ gene copies mL^{-1} (B11) followed by an even more pronounced decline and stabilization at low levels from B14 onwards. Best evaluation of nitrifier dynamics can be achieved by pairwise comparison of the relative abundances as given in Fig. 7 and Figure S4. The ratio between AerAOB and AnAOB ranged between 2.3 (B4) and 375 (B7), with lowest values and thus highest AnAOB numbers for the B stage at samplings B4 (2.3), B5 (7.6), B12 (7.8) and B15 (14.3), respectively. In the sidestream, a clearly narrower and stable ratio of AerAOB/AnAOB with an average value of 0.7 ± 0.7 (SL1-SL17) was observed.

The ratio of gene copy numbers of AerAOB to NOB changed from an initial value of 0.6 (B1) to a subsequently AerAOB dominated community (B2-B6: 7.37 ± 7.84). From B7-B10, again NOB were dominant

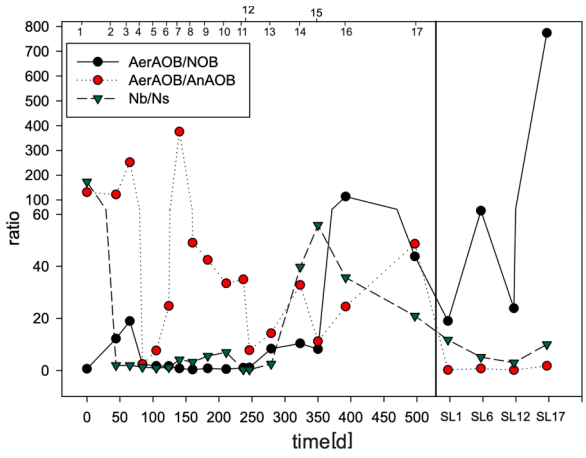

Fig. 7. Determination of AerAOB/AnAOB, AerAOB/NOB and Nb/Ns ratios, based on 16S rRNA genes abundances. The lower X-Axis depicts the time-frame of the whole monitoring campaign in days and the upper X-Axis highlights the seventeen sampling events. Right box summarizes the four sampling points performed for SL-samples (1, 6, 12 and 17). For SL-samples X-Axis does not reflect the correct time span of the experiment. Please note that the interval of the Y-axis is varying.

(0.57 ± 0.21). Thereafter the ratio increased (26.6 ± 41), peaking at B16 with 113:1 and eventually comparable to the sidestream. When looking at the NOB community in more detail, a general dominance of Nb was detected throughout the sampling period, with two exceptions, namely sampling B5 (Nb:Ns of 0.93) and the sudden Ns increase at the sampling B11 (Nb:Ns of 0.30) and B12 (Nb:Ns of 0.27). After sampling B12 the Nb dominance was even more pronounced (Nb:Ns of 38.1 ± 14.4). In the sidestream a constant predominance of Nb was observed (Nb:Ns of 7.43 ± 4.08), although at lower ratios as discovered in B13-B17. A more thorough discussion of obtained results is given in the supplementary material.

3.6. Qualitative consortium analysis

In the mainstream the bacterial community was mainly composed of *Proteobacteria, Bacteroidetes, Actinobacteria, Chloroflexi, Saccharibacteria, Planctomyces, Firmicutes*, and *Nitrospirae* in descending relative abundance (Fig. 8). The number of these eight core phyla was only exceeded at B11-B12 and B15–17 with the emergence or strong increase of *Chlorobi, Chloroflexi, Synergistes* and *Spirochaetes*. The sidestream exhibited a similar but more stable core population, the appearance of novel phyla or rise of *Chloroflexi* was however not observed, instead a relatively higher share of *Saccharibacteria* was noted. The AnAOB population was clearly dominated by Candidatus *Brocadia fulgida.*

Monitoring the evolution of key groups via DGGE rendered the following main outcomes: i) samples of time point B1 (control) always grouped into a separate cluster (Figure S10 and Figure S11), ii) banding patterns for Nb and AerAOB were different for sidestream and mainstream samples (Figure S10 and Figure S11) iii) Nb showed the highest diversity (band number) peaking at B13 (Figure S12). The supplementary material gives more details on the qualitative consortium analyses (also refer to Figure S8 and Figure S9).

3.7. Community evolution over time

The principal component analysis (Fig. 9) depicted a clustering of sampling phases that was not essentially driven by ambient temperatures (e.g. samples of warm or cold seasons did not group together), but rather by the duration of the bioaugmentation campaign itself (i.e. clusters: B1; B2-B6; B7-B10; B11-B12; B13-B17). The group that is obviously located against the general trend of moving from the left to the right on axis 1 over time is sampling B7-B10, which is characterised by decreasing ambient temperatures and influent load (see Fig. 1). The most influential microbial parameters for sample differentiation were *Nitrospira*-, AnAOB-, AerAOB- qPCR copy numbers, and AnAOB area. This general sample evolution was also corroborated by a PCA ordination on replicate samples and including only the variables pH, EC, $1/DOM_{ms}$, α_{250}, α_{365} (see Figure S13). The β-diversity, based on sequencing

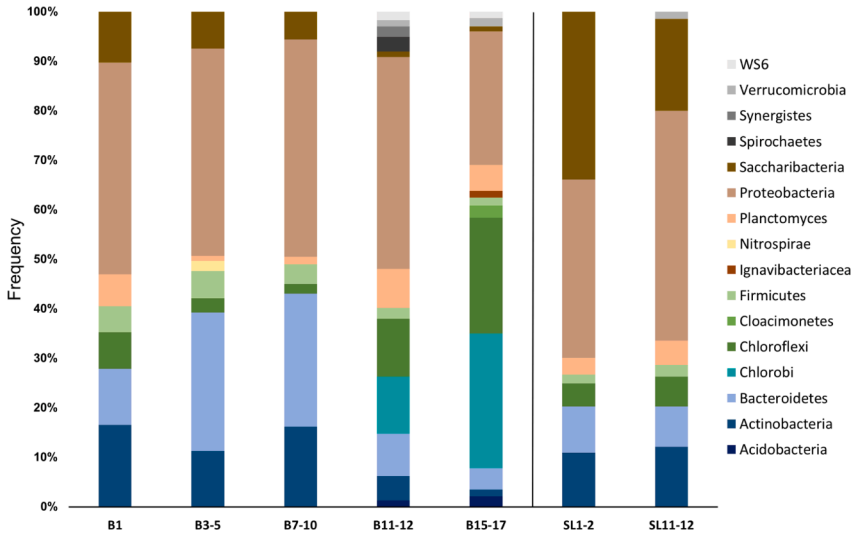

Fig. 8. Evolution of the bacterial community in the mainstream (B) and DEMON (SL) at phylum level (> 1% of total abundance), based on 16S amplicon sequencing results of the V6 region. Specific experimental phases/sampling times were combined, and are summarized in the sample names.

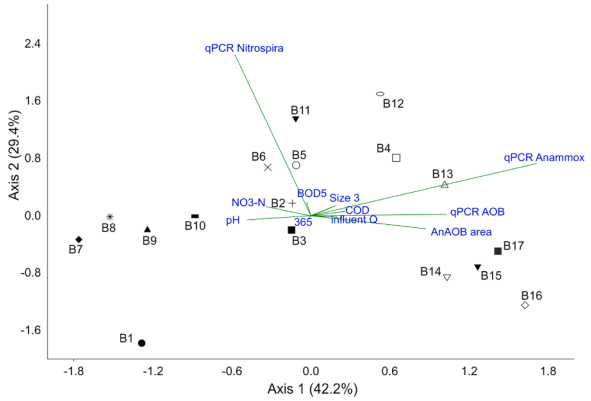

Fig. 9. Principal component analysis of microbial community characteristics for B-samples over time. The numbers next to the symbols represent the seventeen sampling campaigns that were performed (B1-B17). The variance explained by axis 1 and 2 were 42.2% and 29.4%, respectively. Only variables with a correlation with either axes > 0.55 or < −0.55 are shown.

data, shows a similar pattern (see Figure S14). The control sampling prior to seeding (B1) aligns on the first axis with the sidestream samples (SL1–2; SL11–12), whilst the earlier samplings (B3–5 and B7–10) group closely together and eventually later samplings (B11–12 and B15–17) distinctively move apart on the first axis that is accounting for 72.5% of the total variance (Figure S14). This clustering is basically due to higher relative numbers of *Saccharibacteria* within sidestream communities (shift on axis 2) and higher α-diversity along with a rising dominance of *Chlorobi* and *Chloroflexi* in mainstream samples at the later sampling events (i.e. drastic shift on the first coordinate).

Positive correlations were found for parameters AnAOB B-UF area with NO_2, *Nb/Ns* and heme concentration, with 0.65, 0.63 and 0.78, respectively (Table S6). Furthermore AerAOB was positively correlated to AnAOB (0.73) and negatively to *Nitrobacter* (−0.62) and NO_3 (−0.69). Extended results can be found in the supplementary material in Table S6.

4. Discussion

4.1. Process changes after implementation of mainstream deammonification

This full-scale and long-term bioaugmentation campaign of DEMON® sidestream biomass to the mainstream, combined with the testing of different DO-regimes (i.e. carousel-type aeration leading to a DO-range of 0.00 to 0.55 mg L^{-1} - for more information on this DO-regimes refer to (Wett et al., 2015) - led to a clear shift from conventional nitrification to partial nitritation within approximately eight months. The regular transfer of sidestream biomass did not affect the operation of the DEMON® tank. Indeed, values of the preceding year could even be exceeded with 96% as to 95% of mean ammonium-elimination. *Ex-situ* activity tests indicate that nitrate formation was inhibited under experimental conditions. In addition, it is noteworthy to point out the simultaneous anaerobic ammonia- and nitrite depletion, although concomitant ammonia removal seems to be neglectable. Of course, ammonia- and nitrite concentrations of the mainstream were not as high as in the *ex-situ* activity measurements, but elevated effluent nitrite levels after sampling B11 that prevailed until B15 indicate that nitrite shunt activities had also taken place *in-situ* in the mainstream. A recent study on a three-year lasting seeding of AnAOB biomass towards the mainstream of a full-scale WWTP in Denmark without additional retention of AnAOB biomass in the mainstream could only attribute ca. 1% contribution of anammox activity to the total nitrogen removal and no direction towards nitritation/denitritation was achieved (Kamp et al., 2019). In the study presented here, and as reflected by the simultaneous depletion of nitrite and ammonia (Fig. 4), the seeding and especially retention of AnAOB via hydrocyclones had a clear impact on the microbial community without negatively affecting the performance of neither mainstream nor sidestream. This is especially intriguing, as simultaneous depletion of both nitrogen species was observed at ambient temperatures clearly below 15 °C, a range generally considered unfavorable for deammonification (Cao et al., 2017). In fact, the volumetric NRR but also biomass-specific NRR could even be increased throughout the monitoring campaign (see Table S7).

4.2. Microbial community dynamics

The effect of sidestream bioaugmentation to the mainstream is also reflected in the microbial consortium. The sampling campaign covered several seasons and in the case of the WWTP AIZ, also tourism-affected

phases. Under standard conditions (i.e. conventional mainstream nitrification/denitrification) microbial consortia are rather expected to group according to the same operating conditions, i.e. seasons. In this study, samples from the same season did not cluster together (Fig. 9), suggesting that a more substantial change took place. A study on seasonal changes in waste activated sludge of a WWTP in a temperate climate zone by Johnston et al. (2019) reported significant differences between the waste activated sludge (WAS) microbiota of the same seasons of two consecutive years. Still same seasons (in that case summer) were more similar to each other than to any other season, combined however, with a general annual drift of the WAS community (Johnston et al., 2019). In our study, samples from same seasons were clearly separated, and apart from B7-B10 (autumn), a constant drift over time was noticeable that is therefore most probably attributed to the bioaugmentation. According to sequencing data, the most obvious change occurred around B11-B12, when considerable populations of *Chloroflexi* and *Chlorobi* were increased or appeared, respectively (see also Figure S14). The group of *Planctomycetes* showed also a higher abundance at these time points, pointing at a combined enrichment of all three groups through the seeding process, a trend that was perceivable for approximately eight months until the end of the monitoring campaign. This trend was not observed in the sidestream and this points at the emergence of a very specialized microbial consortium, adapted to anoxic conditions, most probably fostered through the specific aeration regime in the mainstream and the increase of granular biomass, also harbouring anoxic niches. A simultaneous enrichment of AnAOB, together with members of *Chloroflexi* under mainstream conditions, was also observed in a partial nitritation/anammox experiment (Yang et al., 2018) and close interaction of both groups is further suggested by (Ali et al., 2020; Annavajhala et al., 2018). A prior lab experiment with the same DEMON® seeding source also identified *Chloroflexi* as important player, especially in granular anammox biomass (Park et al., 2010a). This microbial group is thought to feed on cell decay of autotrophs and their filamentous cell shape is believed to facilitate the generation and/or maintenance of the granular structures (Kragelund et al., 2011). In our study, a very dominant cluster of the class *Anaerolineae*, with one OTU comprising even 10.5% of all reads at B15–17 was detected. This group of "semi-syntrophic" (Narihiro et al., 2012), fermentative bacteria can be considered as core class of anaerobic digestion processes. The exact role or specific conditions within the mainstream that lead to the clear emergence of this class needs to be further investigated. According to Xia and coworkers, it is the high ability to generate type IV pili that makes *Anaerolineae* potent candidates for cell adhesion, necessary for biofilm generation and direct interspecies electron transfer (DIET) (Xia et al., 2016).

Members of the *Chlorobi* that were detected in the mainstream from B11 onwards might have played a pivotal role in the degradation of extracellular polymeric substances (EPS), typically present in and bonding the anammox granules (Wang et al., 2020). These EPS could act as secure carbon source for these heterotrophs and in return members of the *Chlorobi* could help to reduce nitrate produced by AnAOB, to nitrite, thus improving overall conditions for AnAOB growth and metabolic activity (Annavajhala et al., 2018; Lawson et al., 2017; Park et al., 2010b). It is intriguing however, that this group was hardly detectable in the sidestream ($< 0.15\%$) but out of the 30 Chlorobi-associated OTUs one single OTU that could be phylogenetically assigned to the class of SJA-28, accounted for over 20% of total reads at B15–17. The exact role of this important player within the mainstream microbiota needs to be further elucidated. Possibly, especially mainstream conditions fostered this group, but also members of the *Ignavibacteriacea, Acidobacteria, Synergistes* or *Spirochaetes* that were not detectable in SL, eventually emerged in the B-stage. In contrast, *Planctomycetes* and *Chloroflexi* were clearly present in the SL-samples.

The group of *Planctomycetes* was also present at a considerable abundance at B1, raising the question of an autochthonous presence of AnAOB in the WAS. This finding is corroborated by the particle tracking and heme quantification that were able to detect, although at very low numbers/concentrations granules/heme, respectively, in the B1-sample. To our experience background heme concentrations of WWTP that are not influenced by an on-site anammox process range around 0.08 μmol L^{-1}, whereas 0.85 μmol L^{-1} (although measured in the B-UF1- and not B1-sample) were detected at WWTP AIZ. This higher natural presence of AnAOB can be explained by the on-site installation of the DEMON® tank already in 2004 and partial treatment of sidestream excess sludge via the mainstream. Still the initial AnAOB population of the mainstream was negligible regarding nitrogen removal processes and a real change occurred only once the regular seeding and hydrocyclone-retention was started. This fact is also confirmed by the fact that B1-samples of all investigated groups (AerAOB, AnAOB, Ns and Nb) form a separate cluster in the DGGE-analyses at the first time point.

4.3. Bioaugmentation effect on key players of the nitrogen cycle in the mainstream

The most obvious fact was the increase in the AerAOB/NOB ratio after B12 that further increased and remained at elevated levels until the end of the sampling campaign. This ratio was then comparable with the one encountered in the SL and ratios > 1 can, according to our findings, be considered essential for partial nitritation. Interestingly, at the first occurrence of simultaneous ammonia- and nitrite depletion (activity measurement B12; Fig. 4), the ratio AerAOB/NOB was only 1.1. A population shift towards AerAOB was already observed earlier in the monitoring campaign, around B2-B6, however at these stages not coinciding with higher nitrite levels in the mainstream. The AnAOB abundance (qPCR-based) was also clearly increased at these earlier stages, even though such increase was accompanied by low heme concentration in B-UF samples (Figure S7), pointing towards a still less active or less adapted AnAOB biomass (Ali et al., 2013; Podmirseg et al., 2015). Another difference between these two phases relied on high temperature and low-strain phase for the earlier time points (B2-B6), as compared to low temperatures and high strain phase at sampling B11-B12, possibly facilitating nitrite accumulation in the mainstream and thus deammonification. *Ex-situ* activity measurements that could have further proved if an earlier direction towards nitrification occured, however, were only included from sampling B5 onwards.

The higher nitrite levels were eventually achieved through an operating mode that allowed for transient anoxic conditions along the flow-path (Wett et al., 2015). Also, earlier modeling-approaches confirmed that a rather rapid transition between high- and low DO conditions, instead of constant low DO-levels eventually leads to NOB repression (Wett et al., 2013).

It can definitely be stated that the microbial group that was most affected by the operating scheme in the mainstream was the NOB. This effect took place at B12 and manifested itself in a drastic drop of *Nitrospira*, whereas the *Nitrobacter* population remained stable. Our findings corroborate an extensive lab-scale study that compared microbial communities in partial nitritation and conventional nitrification systems (Zhao et al., 2018). Also there, a shift towards partial nitritation is accompanied by a dominance of *Nitrobacter*, whereas conventional operational schemes allow for an equilibrium of both genera (Zhao et al., 2018). This shift might be explained by the physiological differences of both NOBs, as *Nitrospira* exhibit high substrate-affinity and slow growth rate, and *Nitrobacter* show low-substrate affinity and higher growth-rate (Park et al., 2017), favouring the dominance of the latter, especially at elevated nitrite concentrations (i.e. around B12). This eventual predominance of Nb was accompanied by an increase in Nb diversity at stable cell numbers. Probably, environmental conditions fostered the emergence of more adapted *Nitrobacter* strains. As opposed to sidestream systems, facing high levels of free ammonia (FA), the range of FA within the mainstream (0.16 ± 0.2 mg FA L^{-1}) might not have been high enough to act as further NOB-suppressing factor (Cao et al., 2017; Poot et al., 2016).

It remains uncertain if a concomitant activity of comammox within the mainstream system took place. So far this group has been linked to an oligotrophy, but recent findings suggest a very high habitat versatility and non-neglectable role of comammox bacteria, especially at lower ammonia nitrogen- and DO-levels (Annavajhala et al., 2018; Kits et al., 2017; Luo et al., 2022; Yung-Hsien and Jer-Horng, 2021). In this study, 16S rRNA gene analysis for comammox *Nitrospira*-related OTUs did not allow for phylogenetic classification down to species-level, thus a detection of distinct comammox-bacteria was impeded but should be a focus of future studies.

Candidatus *Nitrotoga*, a cold-adapted NOB of the group of Betaproteobacteria that can also be enriched from activated sludge of WWTP with very similar average annual temperatures, was not detected in our study (Alawi et al., 2007).

The question remains, if the dominance of *Nitrobacter* within the NOB population is the key to the direction of the mainstream towards combined NOB suppression and nitritation/deammonification, or if this was only one possible approach that was valid for our study design and further intensified through the higher Nb abundance of the seeding source.

Nevertheless, and summarizing, the combination of successful NOB suppression and bioaugmentation of AnAOB/AerAOB from the sidestream to the mainstream raised the potential of the microbiota to increased nitrite generation of up to 86% of total NO_x-N (B16) after a time of eight months (starting at ca. B12).

4.4. Evaluation of the AnAOB enrichment strategy

The success of the two chosen enrichment and retention strategies (i.e. frequent transfer of excess biomass from the sidestream (SL-OF) and mainstream hydrocyclone operation) could be demonstrated via all monitored parameters (qPCR, heme quantification, particle tracking) and partly via the activity measurements. They all exhibited a very similar pattern, corroborating a trend with peaks around B12-B14 and elevated values thereafter. It would be an interesting task to compare AnAOB-related gene expression profiles as shown previously (Park et al., 2010b, 2015) with heme concentration, to see to which extent activity and not only presence is captured by this parameter.

Although AnAOB granule size varied significantly, it showed a constant increase of relative abundance for the mid-size fractions 0.1–0.2 and 0.2–0.3 mm over time. It has been stated by several authors that not the granule size, but rather the total number of granules and especially the smaller granules with large surface area render the process more effective (Cao et al., 2017). This might be due to faster proliferation, larger mass transfer and general activity of suspended or free AnAOB biomass (Cao et al., 2017). In contrast to this, other authors stated that larger granules – especially when shielded with an AerAOB rim, bear higher anammox activity rates than small aggregates (Nielsen et al., 2005; Vlaeminck et al., 2010). Due to the relatively high doubling time of approximately eleven days under ideal conditions and $>$ 25 days at temperatures below 20 °C (Xu et al., 2015), sole seeding of biomass from sidestream to mainstream does not seem to have enough impact on AnAOB retention. Comparing results of other full-scale studies, the implementation of the hydrocyclone or similar retention devices (e.g. screens), is regarded a prerequisite for biomass maintenance in the mainstream (Han et al., 2016; Kamp et al., 2019). This might have been the right combination of AnAOB selecting factors, that eventually led to the establishment of a distinct AnAOB population, accompanied by an increase in the volumetric NRR, even throughout the colder winter season as reflected by comparison of mean volumetric NRR values of the first phase (B1-B10; 42.6 $\pm$ 13.3 g m^{-3} d^{-1}) and the second phase (B11-B17; 81.0 $\pm$ 17.9 g m^{-3} d^{-1}) of this monitoring campaign. Focusing on the quantification results, it seems for the system studied that AnAOB abundance of approximately $>$ 1.13 $\pm$ 0.07 μmol heme L^{-1} or ca. 10^5 AnAOB 16S rRNA gene copies per mL^{-1} are necessary for a direction towards a noticeable deammonification activity within the mainstream. Equally, a relative abundance of AnAOB of at least 0.1% of the total bacterial population was necessary to observe simultaneous ammonia and nitrite depletion and reduced nitrate generation potential.

5. Conclusion

The initial microbial community of the mainstream responded to operational changes and displayed a noticeable switch in its functional potential as displayed via *ex-situ* activity tests. The abundance of the AnAOB population was eventually large enough to detect deammonification at later time points, and seeding from sidestream to mainstream had a positive effect on overall nitrogen removal efficiency. Volumetric- and biomass-specific NRR experienced nearly a doubling in the mainstream pointing at a robust process performance at reduced aeration costs due to the optimized carousel-type aeration regime. Suppression of NOB was expressed by elevated nitrite concentrations and went along with simoultaneous AnAOB activity (significant heme:NO_2 correlation). In our study, Ns-related NOB out-competition was basically achieved by continued feeding of sidestream biomass, enriched in AerAOB and Nb. Interestingly, the repression of NOB occurred under unfavorable plant operational conditions, i.e. cold winter season and high organic load. Thus a combination of both, the bioaugmentation strategy, combined with the prevailing higher ammonia- and nitrite concentrations might have further promoted this observed switch. More research is needed on potential enrichment approaches of AnAOB biomass in the mainstream (e.g. hydrocyclone versus screen impact on the microbiota) and fine-tuning of selective suppression/promotion of specific microbial players, combined with a monitoring of functional gene expressions patterns. In addition the role of comammox within these settings needs further elucidation.

Author contribution statement

The study design was developed by BW, MH (AIZ WWTP), SMP, MGB, and HI; sampling performed by SMP, MGB, MM and MH; SMP and MGB coordinated the laboratory work; analyses were done by SMP, MGB, MM, MH, HP, TP; data analysis and statistics were conducted by SMP, MGB, BS; sequencing was performed by HP, bioinformatic analyses conducted by SMP, HP and MGB; SMP generated the figures and tables; the manuscript was written by SMP and partly by MGB and MM; BS provided valuable statistical help and feedback on manuscript structure; critical reviewing of the manuscript was performed by all authors and all authors approve the submitted version of this manuscript.

Declaration of Competing Interest

None to declare.

Acknowledgements

This project is jointly funded by the District of Columbia Water and Sewer Authority (DCWater), Washington DC, the Hampton Roads Sanitation District (HRSD), Virginia, the Achental-Inntal-Zillertal Waterboard (AIZ), Austria and the Water Environment Research Federation (WERF) through a grant by the United States Environmental Protection Agency. We would like to thank the whole team of the WWTP AIZ Strass (Austria) for their help and agreeable collaboration throughout the whole sampling campaign and thereafter and the Innovation-group of DC Water for continuous exchange of experience. Further thanks go to Kärt Kanger for her highly appreciated help during several sampling events in the course of her internship. MGB acknowledges support by the Programa Ramón y Cajal (RYC-2016–21231; Ministerio de Economía y Competitividad).

BS was partially supported through the guest professorship awarded by the University of Innsbruck and Slovenian Research Agency (SRA

Programme P2–0180: Water Science and Technology, and Geotechnical Engineering: Tools and Methods for Process Analyses and Simulations, and Development of Technologies). We thank Paul Fraiz Martinez for the thorough linguistic check of the manuscript. Moreover we thank the two anonymous reviewers for their constructive comments on this manuscript.

Supplementary materials

Supplementary material associated with this article can be found, in the online version, at doi:10.1016/j.watres.2022.118517.

References

Alawi, M., Lipski, A., Sanders, T., Pfeiffer, E.M., Spieck, E., 2007. Cultivation of a novel cold-adapted nitrite oxidizing betaproteobacterium from the Siberian Arctic. ISME J. 1 (3), 256–264.

Ali, M., Chai, L.Y., Tang, C.J., Zheng, P., Min, X.B., Yang, Z.H., Xiong, L., Song, Y.X., 2013. The increasing interest of ANAMMOX research in China: bacteria, process development, and application. Biomed. Res. Int. 2013, 134914.

Ali, M., Shaw, D.R., Albertsen, M., Saikaly, P.E., 2020. Comparative Genome-Centric Analysis of Freshwater and Marine ANAMMOX Cultures Suggests Functional Redundancy in Nitrogen Removal Processes. Front. Microbiol. 11, 1637.

Annavajhala, M.K., Kapoor, V., Santo-Domingo, J., Chandran, K., 2018. Structural and Functional Interrogation of Selected Biological Nitrogen Removal Systems in the United States, Denmark, and Singapore Using Shotgun Metagenomics. Front. Microbiol. 9, 2544.

Bai, Y., Sun, Q., Wen, D., Tang, X., 2012. Abundance of ammonia-oxidizing bacteria and archaea in industrial and domestic wastewater treatment systems. FEMS Microbiol. Ecol. 1–8.

Broda, E., 1977. Two kinds of lithotrophs missing in nature. Z. Allg. Mikrobiol. 17 (6), 491–493.

Cao, Y., van Loosdrecht, M.C., Daigger, G.T., 2017. Mainstream partial nitritation-anammox in municipal wastewater treatment: status, bottlenecks, and further studies. Appl. Microbiol. Biotechnol. 101 (4), 1365–1383.

Christensson, M., Ekstrom, S., Andersson Chan, A., Le Vaillant, E., Lemaire, R., 2013. Experience from start-ups of the first ANITA Mox plants. Water Sci. Technol. 67 (12), 2677–2684.

Daims, H., Lebedeva, E.V., Pjevac, P., Han, P., Herbold, C., Albertsen, M., Jehmlich, N., Palatinszky, M., Vierheilig, J., Bulaev, A., Kirkegaard, R.H., von Bergen, M., Rattei, T., Bendinger, B., Nielsen, P.H., Wagner, M., 2015. Complete nitrification by Nitrospira bacteria. Nature 528 (7583), 504–509.

De Clippeleir, H., Vlaeminck, S.E., De Wilde, F., Daeninck, K., Mosquera, M., Boeckx, P., Verstraete, W., Boon, N., 2011. One-stage partial nitritation/anammox at 15 °C on pretreated sewage: feasibility demonstration at lab-scale. Applied Microbiology Biotechnology 97 (23), 10199–10210.

Gottshall, E.Y., Bryson, S.J., Cogert, K.I., Landreau, M., Sedlacek, C.J., Stahl, D.A., Daims, H., Winkler, M., 2021. Sustained nitrogen loss in a symbiotic association of Comammox Nitrospira and Anammox bacteria. Water Res. 202, 117426.

Hammer, O., Harper, D., Ryan, P., 2001. Paleontological Statistics Software Package for Education and Data Analysis. Palaeontologia Electronica 4, 1–9.

Han, M., Vlaeminck, S.E., Al-Omari, A., Wett, B., Bott, C., Murthy, S., De Clippeleir, H., 2016. Uncoupling the solids retention times of flocs and granules in mainstream deammonification: a screen as effective out-selection tool for nitrite oxidizing bacteria. Bioresour. Technol. 221, 195–204.

Hendrickx, T.L., Wang, Y., Kampman, C., Zeeman, G., Temmink, H., Buisman, C.J., 2012. Autotrophic nitrogen removal from low strength waste water at low temperature. Water Res. 46 (7), 2187–2193.

Hoekstra, M., Geilvoet, S.P., Hendrickx, T.L.G., van Erp Taalman Kip, C.S., Kleerebezem, R., van Loosdrecht, M.C.M., 2019. Towards mainstream anammox: lessons learned from pilot-scale research at WWTP Dokhaven. Environ. Technol. 40 (13), 1721–1733.

Hupfauf, S., Etemadi, M., Fernandez-Delgado Juarez, M., Gomez-Brandon, M., Insam, H., Podmirseg, S.M., 2020. CoMA - an intuitive and user-friendly pipeline for amplicon-sequencing data analysis. PLoS ONE 15 (12), e0243241.

Jetten, M., Van Niftrik, L., Strous, M., 2009. Biochemistry and molecular biology of anammox bacteria. Crit. Rev. Biochem. Mol. Biol. 44, 65–84.

Johnston, J., LaPara, T., Behrens, S., 2019. Composition and Dynamics of the Activated Sludge Microbiome during Seasonal Nitrification Failure. Sci. Rep. 9 (1), 4565.

Kalyuzhnyi, S.V., Gladchenko, M.A., Kang, H., Mulder, A., Versprille, A., 2008. Development and optimisation of VFA driven DEAMOX process for treatment of strong nitrogenous anaerobic effluents. Water Sci. Technol. 57 (3), 323–328.

Kamp, A., Ottosen, L.D.M., Thogersen, N.B., Revsbech, N.P., Thamdrup, B., Andersen, M. H., 2019. Anammox and partial nitritation in the mainstream of a wastewater treatment plant in a temperate region (Denmark). Water Sci. Technol. 79 (7), 1397–1405.

Kartal, B., van Niftrik, L., Keltjens, J.T., Op den Camp, H.J., Jetten, M.S., 2012. Anammox–growth physiology, cell biology, and metabolism. Adv. Microb. Physiol. 60, 211–262.

Kits, K.D., Sedlacek, C.J., Lebedeva, E.V., Han, P., Bulaev, A., Pjevac, P., Daebeler, A., Romano, S., Albertsen, M., Stein, L.Y., Daims, H., Wagner, M., 2017. Kinetic analysis of a complete nitrifier reveals an oligotrophic lifestyle. Nature 549 (7671), 269–272.

Kragelund, C., Thomsen, T.R., Mielczarek, A.T., Nielsen, P.H., 2011. Eikelboom's morphotype 0803 in activated sludge belongs to the genus Caldilinea in the phylum Chloroflexi. FEMS Microbiol. Ecol. 76 (3), 451–462.

Lackner, S., Gilbert, E.M., Vlaeminck, S.E., Joss, A., Horn, H., van Loosdrecht, M.C., 2014. Full-scale partial nitritation/anammox experiences–an application survey. Water Res. 55, 292–303.

Lawson, C.E., Wu, S., Bhattacharjee, A.S., Hamilton, J.J., McMahon, K.D., Goel, R., Noguera, D.R., 2017. Metabolic network analysis reveals microbial community interactions in anammox granules. Nat. Commun. 8, 15416.

Le, T., Peng, B., Su, C.Y., Massoudieh, A., Torrents, A., Al-Omari, A., Murthy, S., Wett, B., Chandran, K., DeBarbadillo, C., Bott, C., De Clippeleir, H., 2019. Impact of carbon source and COD/N on the concurrent operation of partial denitrification and anammox. Water Environment Research 91 (3), 185–197.

Li, X., Klaus, S., Bott, C., He, Z., 2018. Status, Challenges, and Perspectives of Mainstream Nitritation-Anammox for Wastewater Treatment. Water Environ. Res. 90 (7), 634–649.

Lindell, M., Granéli, W., Tranvik, L., 1995. Enhanced bacterial growth in response to photochemical transformation of dissolved organic matter. Limnol. Oceanogr. 40, 195–199.

Liu, L., Ji, M., Wang, F., Wang, S., Qin, G., 2020. Insight into the influence of microbial aggregate types on nitrogen removal performance and microbial community in the anammox process - A review and meta-analysis. Science of The Total Environment 714, 136571.

Luo, S., Peng, Y., Liu, Y., Peng, Y., 2022. Research progress and prospects of complete ammonia oxidizing bacteria in wastewater treatment. Frontiers of Environmental Science and Engineering 16, 123.

Mardanov, A.V., Beletsky, A.V., Ravin, N.V., Botchkova, E.A., Litti, Y.V., Nozhevnikova, A.N., 2019. Genome of a Novel Bacterium "Candidatus Jettenia ecosi" Reconstructed From the Metagenome of an Anammox Bioreactor. Front. Microbiol. 10, 2442.

Narihiro, T., Terada, T., Ohashi, A., Kamagata, Y., Nakamura, K., Sekiguchi, Y., 2012. Quantitative detection of previously characterized syntrophic bacteria in anaerobic wastewater treatment systems by sequence-specific rRNA cleavage method. Water Res. 46 (7), 2167–2175.

Nielsen, M., Bollmann, A., Sliekers, O., Jetten, M., Schmid, M., Strous, M., Schmidt, I., Larsen, L.H., Nielsen, L.P., Revsbech, N.P., 2005. Kinetics, diffusional limitation and microscale distribution of chemistry and organisms in a CANON reactor. FEMS Microbiol. Ecol. 51 (2), 247–256.

Park, H., Rosenthal, A., Jezek, R., Ramalingam, K., Fillos, J., Chandran, K., 2010a. Impact of inocula and growth mode on the molecular microbial ecology of anaerobic ammonia oxidation (anammox) bioreactor communities. Water Res. 44 (17), 5005–5013.

Park, H., Rosenthal, A., Ramalingam, K., Fillos, J., Chandran, K., 2010b. Linking Community Profiles, Gene Expression and N-Removal in Anammox Bioreactors Treating Municipal Anaerobic Digestion Reject Water. Environ. Sci. Technol. 44 (16), 6110–6116.

Park, H., Sundar, S., Ma, Y., Chandran, K., 2015. Differentiation in the microbial ecology and activity of suspended and attached bacteria in a nitritation-anammox process. Biotechnol. Bioeng. 112 (2), 272–279.

Park, M.R., Park, H., Chandran, K., 2017. Molecular and Kinetic Characterization of Planktonic Nitrospira spp. Selectively Enriched from Activated Sludge. Environ. Sci. Technol. 51 (5), 2720–2728.

Podmirseg, S.M., Pumpel, T., Markt, R., Murthy, S., Bott, C., Wett, B., 2015. Comparative evaluation of multiple methods to quantify and characterise granular anammox biomass. Water Res. 68, 194–205.

Podmirseg, S.M., Waldhuber, S., Knapp, B.A., Insam, H., Goberna, M., 2019. Robustness of the autochthonous microbial soil community after amendment of cattle manure or its digestate. Biol Fert Soils 55 (6), 565–576.

Poot, V., Hoekstra, M., Geleijnse, M.A.A., van Loosdrecht, M.C.M., Perez, J., 2016. Effects of the residual ammonium concentration on NOB repression during partial nitritation with granular sludge. Water Res. 106, 518–530.

Shehzad, A., Liu, J., Yu, M., Qismat, S., Liu, J., Zhang, X.H., 2016. Diversity, Community Composition and Abundance of Anammox Bacteria in Sediments of the North Marginal Seas of China. Microbes Environ 31 (2), 111–120.

Strous, M., Fuerst, J.A., Kramer, E.H.M., Logemann, S., Muyzer, G., van de Pas-Schoonen, K.T., Webb, R., Kuenen, J.G., Jetten, M.S.M., 1999a. Missing lithotroph identified as new planctomycete. Nature 400 (6743), 446–449.

Strous, M., Kuenen, J.G., Jetten, M.S., 1999b. Key physiology of anaerobic ammonium oxidation. Appl. Environ. Microbiol. 65 (7), 3248–3250.

Sun, W., Xia, C., Xu, M., Guo, J., Wang, A., Sun, G., 2014. Diversity and distribution of planktonic anaerobic ammonium-oxidizing bacteria in the Dongjiang River. China. Microbiol Res 169 (12), 897–906.

Szatkowska, B., Paulsrud, B., 2014. The Anammox process for nitrogen removal from wastewater – achievements and future challenges. VANN 49 (2), 186–194.

van Dongen, U., Jetten, M.S., van Loosdrecht, M.C., 2001. The SHARON-Anammox process for treatment of ammonium rich wastewater. Water Sci. Technol. 44 (1), 153–160.

van Niftrik, L., Jetten, M.S., 2012. Anaerobic ammonium-oxidizing bacteria: unique microorganisms with exceptional properties. Microbiol. Mol. Biol. Rev. 76 (3), 585–596.

Vlaeminck, S.E., Terada, A., Smets, B.F., De Clippeleir, H., Schaubroeck, T., Bolca, S., Demeestere, L., Mast, J., Boon, N., Carballa, M., Verstraete, W., 2010. Aggregate size and architecture determine microbial activity balance for one-stage partial nitritation and anammox. Appl. Environ. Microbiol. 76 (3), 900–909.

Wang, D., Wang, Q., Laloo, A., Xu, Y., Bond, P.L., Yuan, Z., 2016. Achieving Stable Nitritation for Mainstream Deammonification by Combining Free Nitrous Acid-Based Sludge Treatment and Oxygen Limitation. Sci. Rep. 6, 25547.
Wang, W., Wang, J., Wang, H., Ma, J., Wu, M., Wang, Y., 2020. Anammox Granule Enlargement by Heterogenous Granule Self-assembly. Water Res. 187, 116454.
WEF/WERF, 2015. Shortcut Nitrogen Removal—Nitrite Shunt and Deammonification. Water Environment Federation.
Wett, B., 2007. Development and implementation of a robust deammonification process. Water Sci. Technol. 56 (7), 81–88.
Wett, B., Murthy, S., Takács, I., Hell, M., Bowden, G., Deur, A., O'Shaughnessy, M., 2007. Key Parameters for Control of DEMON Deammonification Process. Water Practice 1 (5), 1–11.
Wett, B., Omari, A., Podmirseg, S.M., Han, M., Akintayo, O., Gomez Brandon, M., Murthy, S., Bott, C., Hell, M., Takacs, I., Nyhuis, G., O'Shaughnessy, M., 2013. Going for mainstream deammonification from bench to full scale for maximized resource efficiency. Water Sci. Technol. 68 (2), 283–289.
Wett, B., Podmirseg, S.M., Gomez-Brandon, M., Hell, M., Nyhuis, G., Bott, C., Murthy, S., 2015. Expanding DEMON Sidestream Deammonification Technology Towards Mainstream Application. Water Environ. Res. 87 (12), 2084–2089.
Xia, Y., Wang, Y., Wang, Y., Chin, F.Y., Zhang, T., 2016. Cellular adhesiveness and cellulolytic capacity in Anaerolineae revealed by omics-based genome interpretation. Biotechnol. Biofuels 9, 111.
Xu, G., Zhou, Y., Yang, Q., Lee, Z.M., Gu, J., Lay, W., Cao, Y., Liu, Y., 2015. The challenges of mainstream deammonification process for municipal used water treatment. Appl. Microbiol. Biotechnol. 99 (6), 2485–2490.
Yang, Y., Zhang, L., Cheng, J., Zhang, S., Li, X., Peng, Y., 2018. Microbial community evolution in partial nitritation/anammox process: from sidestream to mainstream. Bioresour. Technol. 251, 327–333.
Yeshi, C., Hong, K.B., van Loosdrecht, M.C., Daigger, G.T., Yi, P.H., Wah, Y.L., Chye, C.S., Ghani, Y.A., 2016. Mainstream partial nitritation and anammox in a 200,000 m3/day activated sludge process in Singapore: scale-down by using laboratory fed-batch reactor. Water Sci. Technol. 74 (1), 48–56.
Yung-Hsien, S., Jer-Horng, W., 2021. Comammox Nitrospira Species Dominate in an Efficient Partial Nitrification−Anammox Bioreactor for Treating Ammonium at Low Loadings. Environmental Science and Technology 55, 2087–2098.
Zhang, M., Wang, S., Ji, B., Liu, Y., 2019. Towards mainstream deammonification of municipal wastewater: partial nitrification-anammox versus partial denitrification-anammox. Sci. Total Environ. 692, 393–401.
Zhao, Z.R., Luo, J.X., Jin, B., Zhang, J.Y., Li, B., Ma, B., An, X.Y., Zhang, S.J., Shan, B.Q., 2018. Analysis of Bacterial Communities in Partial Nitritation and Conventional Nitrification Systems for Nitrogen Removal. Sci Rep-Uk 8.